

Transforming an oxygen-tolerant [NiFe] uptake hydrogenase into a proficient, reversible hydrogen producer†

Cite this: DOI: 10.1039/c3ee43652g

Bonnie J. Murphy,^a Frank Sargent^b and Fraser A. Armstrong^{*a}

Many hydrogenases are highly electroactive when attached to an electrode, and most exhibit reversible $2\text{H}^+/\text{H}_2$ electrocatalysis, *i.e.* only a minuscule overpotential is required to drive the reaction in either direction. A notable exception is an important class of membrane-bound O_2 tolerant [NiFe] hydrogenases that appear only to catalyse H_2 oxidation (the uptake reaction), at a substantial overpotential and with little activity for H_2 production, yet possess an active site that is structurally very similar to that of standard, reversible [NiFe] hydrogenases. In a discovery providing important insight into this puzzle, we show that the O_2 -tolerant [NiFe] hydrogenase (Hyd-1) from *E. coli* converts into a reversible electrocatalyst as the pH is lowered from 8 to 3 and becomes an efficient H_2 producer below pH 4. The transformation to a reversible electrocatalyst is not due, trivially, to the higher substrate (H^+_{aq}) availability at low pH but to a large shift in the enzyme's catalytic bias. Systematic investigations provide compelling evidence that the factor controlling this behaviour is the distal [4Fe–4S] cluster, a spectroscopically elusive site that provides the natural entry point for electrons into the enzyme. In *E. coli* cells, Hyd-1 is located in the periplasmic (extracytoplasmic) compartment and thus, being exposed to the pH extremes of the gastrointestinal tract or the external environment, is a potential catalyst for H_2 production by these bacteria. In a wider context, the observation and proposal are highly relevant for biohydrogen production and catalysis.

Received 6th November 2013
Accepted 13th January 2014

DOI: 10.1039/c3ee43652g

www.rsc.org/ees

Broader context

This paper highlights the importance of enzymes in understanding mechanisms of molecular electrocatalysis – in this case for interpreting the electrochemistry of $2\text{H}^+/\text{H}_2$ interconversion. Microbial O_2 -tolerant hydrogenases are of particular interest as they offer the important possibility of enabling microbes to produce H_2 by modified oxygenic photosynthesis. The best characterised examples – the O_2 -tolerant respiratory [NiFe]-hydrogenases – can oxidise H_2 in air without being inactivated by the action of O_2 on the fragile active site: however, a persistent puzzle has been why these enzymes do not catalyse H_2 production, *i.e.* why they appear to operate exclusively in one direction. The active sites of O_2 -tolerant and standard [NiFe]-hydrogenases have the same ligands and similar atomic arrangements. The results described in this paper show how an O_2 tolerant [NiFe]-hydrogenase transforms smoothly into a proficient H_2 producer as the pH is lowered – an effect that is not trivially due to the increase in proton availability but to an adjustment of the enzyme's redox properties, relative to the pH-sensitive reaction equilibrium potential, to suit H_2 production. As well as being relevant for electrocatalysis and furthering the cause of renewable H_2 , these results may also account for some of the biogenic H_2 produced by bacteria in gastrointestinal systems.

Introduction

The biological hydrogen cycle – the production and oxidation of H_2 by microbes – has wide relevance across biotechnology and

health.^{2,3} Not surprisingly, the extremely high activities of hydrogenases and the nature of their active sites, which contain Fe coordinated by CO and CN^- ligands, with or without Ni, have attracted much attention among chemists. Of the two prominent classes of enzyme, [FeFe] hydrogenases show the highest turnover rates but are notoriously oxygen sensitive, being irreversibly damaged by exposure to even traces of dissolved O_2 .^{4,5} In contrast, most [NiFe] hydrogenases are reversibly inactivated by exposure to O_2 and are usually able to resume catalysis upon reductive reactivation. A special subgroup of the [NiFe] enzymes, termed O_2 -tolerant hydrogenases, has the unique property of catalysing H_2 oxidation in the sustained presence of O_2 , which allows the host organism considerable environmental flexibility as well as identifying these enzymes as candidates for special technology applications. Oxygen-tolerant

^aDepartment of Chemistry, University of Oxford, South Parks Road, Oxford, OX1 3QR, UK. E-mail: fraser.armstrong@chem.ox.ac.uk

^bCollege of Life Sciences, University of Dundee, Dow Street, Dundee DD1 5EH, Scotland, UK

† Electronic supplementary information (ESI) available: Chronoamperometric determination of the product inhibition constant, $K_{\text{I,app}}^{\text{H}_2/\text{H}^+}$ during H_2 production by Hyd-1 at pH 3. Comparison of the H_2 oxidation activity of Hyd-1 at pH 3.0 and 6.0, under 100% H_2 . The onset of H_2 oxidation activity for Hyd-2 as a function of pH. Conceptual demonstration of the cyclic voltammetry trace expected if the limited activity at low potential was due to reductive inactivation of the active site. Cyclic voltammograms for Hyd-1 at low (5 mV s^{-1}) and high (100 mV s^{-1}) scan rate, pH 3.0 and pH 7.0. See DOI: 10.1039/c3ee43652g

membrane-bound hydrogenases (MBHs) from *Ralstonia* species, *Aquifex aeolicus* and *Escherichia coli* have been extensively studied by protein film electrochemistry (PFE), crystallography and spectroscopy, from which a considerable body of mechanistic detail has emerged,^{6–16} in addition to demonstrating the potential utility of O₂-tolerant hydrogen cycling catalysts in novel fuel cells.^{17–22}

All studies to date^{8,23–25} have found that O₂-tolerant MBHs display low or non-existent activity toward H⁺ reduction (H₂ evolution). This is partly because H₂ is a strong product inhibitor, but even under N₂ with a rapidly spinning electrode (to disperse product) only a small H⁺ reduction current is observed. An important mechanistic clue to the poor H₂ producing activity is the observation that a substantial overpotential must be applied before H₂ oxidation commences, as shown by comparing protein film voltammograms recorded for an O₂-tolerant and an O₂-sensitive hydrogenase from *E. coli* (Fig. 1).²⁴ At pH 7 and 10% H₂, the O₂-tolerant hydrogenase-1 (Hyd-1) shows negligible H⁺ reduction activity, and the onset of H₂ oxidation occurs at an overpotential of approximately 0.1 V. These characteristics are conserved across O₂-tolerant MBHs studied to date and are in marked contrast to other hydrogenases, both [NiFe] and [FeFe], that behave as reversible electrocatalysts when attached to an electrode. Explanations accounting for the correlation between the additional overpotential requirement and uni-directionality are discussed further below, but at this stage it is important to be reminded that a catalyst can have no intrinsic bias for reaction direction beyond that dictated by thermodynamics. ‘Bias’ thus refers to comparative activities under different thermodynamic (electrode potential) conditions. It is worth noting that [NiFe]-

hydrogenases are typically biased in the direction of H₂ oxidation (uptake)²⁶ but only for O₂-tolerant MBHs is the bias so extreme as to preclude H⁺ reduction. At high potentials, the H₂ oxidation activity of both Hyd-1 and Hyd-2 is attenuated by conversion to an inactive state, known as Ni-B, which contains a Ni(III)-OH species in the active site, although this species is less stable for Hyd-1.

The [NiFe] membrane-bound hydrogenases (MBHs) are organised minimally as heterodimers, with a large subunit containing the [(Cys-S)₂-Ni-(μ²-Cys-S)₂-Fe(CO)(CN)₂] core of the active site, and a small subunit containing three Fe-S clusters for electron transport to and from the active site. The amino acid sequences and corresponding structures of the active sites of O₂-tolerant and O₂-sensitive [NiFe] hydrogenases thus far examined are very similar, raising the likelihood that any substantial differences in behaviour must originate from elsewhere in the protein. Recent studies^{6,10,14,15,27} have indeed demonstrated the importance of FeS cluster properties in determining O₂ tolerance; specifically, the FeS relay must ensure the rapid transfer of several electrons back to the active site upon its reaction with O₂, thereby forming only Ni-B and avoiding oxidative damage. The structure of Hyd-1 shown in Fig. 2 indicates the positions of the relay centres with respect to the [NiFe] active site and the region of the protein surface close to the more exposed distal cluster (D) across which electrons must enter or leave the enzyme. Mutations of the proximal (P) [4Fe-3S] and/or medial (M) [3Fe-4S] clusters of Hyd-1 severely impair O₂ tolerance but, importantly, have no effect on the onset potential for H₂ oxidation or on the low level of H⁺ reduction,^{6,7} thus establishing that the properties of these buried clusters are not responsible for the lack of reversibility seen for O₂-tolerant enzymes.

A relationship between onset potential and reversibility is predicted for enzymes that possess a redox relay to mediate electron transfer. According to a basic model of hydrogenase electrocatalysis proposed recently by Hexter *et al.*²⁸ the overpotential requirement and catalytic bias (to operate preferentially in a particular direction) of an enzyme adsorbed at an electrode depend on the reduction potential of the centre at which electrons enter or leave the catalyst, relative to the equilibrium potential of the reaction being catalysed. The closer

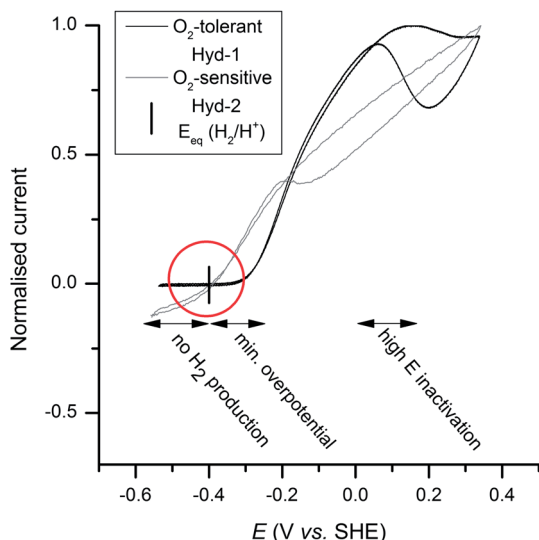


Fig. 1 Electrochemical characteristics of an O₂-tolerant (Hyd-1) vs. an O₂-sensitive hydrogenase (Hyd-2) at pH 7.0 under 10% H₂ at 37 °C. The 2H⁺/H₂ equilibrium potential E_{eq} is marked by the vertical bar. Scan rate 5 mV s⁻¹, electrode rotation rate 2000 rpm. The hysteresis at high potential is due to oxidative inactivation and reactivation through formation of an inactive Ni(III)-OH complex (Ni-B). Labels below voltammograms refer to properties of O₂-tolerant Hyd-1.

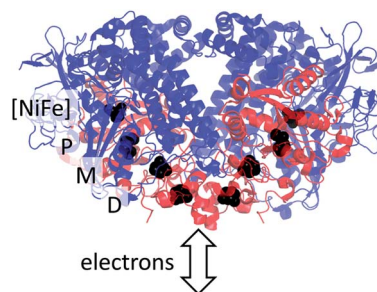


Fig. 2 The structure of Hyd-1 (PDB code 3USC¹) labelling the redox centres in one half of the molecule (a dimer of heterodimers) and the region (arrow) that is most favoured for entry and exit of electrons. [NiFe] = active site, P = proximal [4Fe-3S]^{5+/4+/3+} cluster, M = medial [3Fe-4S]^{1+/0} cluster, D = distal [4Fe-4S]^{2+/1+} cluster.¹

1 together these potentials are, the more reversible is the elec- 1
2 trocatalyst. Based upon structural data, the distal $[4\text{Fe}-4\text{S}]^{2+/1+}$ 2
3 cluster is the natural site at which electrons enter or leave the 3
4 enzyme, but a complication is revealed in recent work by 4
5 Roessler *et al.*¹² who established that the distal $[4\text{Fe}-4\text{S}]$ cluster 5
6 in Hyd-1 is not detectable by standard EPR methods, suggesting 6
7 that the reduced $[4\text{Fe}-4\text{S}]^+$ level has a ground state with $S > 1/2$: a 7
8 similar observation was made for the MBH from *Ralstonia* 8
9 *eutropha*.¹⁵ Although the reduction potential of the distal 9
10 $[4\text{Fe}-4\text{S}]$ cluster in Hyd-1 could not be determined by titrations, 10
11 the model for electrocatalysis predicted a value in the region of 11
12 -0.19 V vs. SHE at pH 6. From studies of the O_2 -tolerant Hase I 12
13 from *A. aeolicus*, Pandelia *et al.*¹⁰ reported that the midpoint 13
14 potential of the distal cluster in that enzyme is -65 mV at pH 14
15 6.4, which is more than 0.2 V more positive than typical O_2 - 15
16 sensitive counterparts. In leading into our work, it is noteworthy 16
17 that $[4\text{Fe}-4\text{S}]$ clusters do not typically show a large pH depen- 17
18 dence of reduction potential, whereas the $2\text{H}^+/\text{H}_2$ reduction 18
19 potential shifts by -0.06 V per pH unit and by -0.03 V per order 19
20 of magnitude increase in H_2 pressure ($\rho(\text{H}_2)$). Consequently, the 20
21 model predicts that Hyd-1 should become a reversible electro- 21
22 catalyst and proficient H_2 producer under more acidic condi- 22
23 tions (assisted by low $\rho(\text{H}_2)$) if the distal cluster is the point of 23
24 entry for electrons and responsible for the observed bias. The 24
25 investigations we now describe give results that are in full 25
26 accordance with this expectation and help to elucidate, in 26
27 general terms, the complex factors determining electrocatalytic 27
28 properties of hydrogenases. The findings not only have specific 28
29 physiological and health implications in regard to H_2 produc- 29
30 tion by *E. coli* throughout the gastrointestinal system but also 30
31 have wider relevance for understanding and optimising bio- 31
32 hydrogen production. 32

35 Methods

33 *E. coli* Hyd-1 was purified as reported previously¹² from strain 33
34 FTH004,²⁹ carrying a $6\times$ His affinity tag at the extreme C- 34
35 terminus of HyaA, expressed from the native locus, using 35
36 0.02% TX-100 detergent. Enzyme samples typically showed 36
37 initial H_2 oxidation activity of 125 s⁻¹ in H_2 -saturated buffer at 37
38 pH 7 and 20 °C, when assayed by following the 604 nm absor- 38
39 bance change of benzyl viologen (BV) due to reduction by Hyd-1 39
40 in 50 mM Tris/HCl, 100 mM NaCl, 25 mM benzyl viologen 40
41 ($\epsilon_{604\text{nm}} = 9.82$ mM⁻¹ cm⁻¹) buffer. This assay certainly under- 41
42 estimates the true activity of Hyd-1 because BV is a poor oxidant. 42
43 Protein film electrochemistry was carried out using an Autolab 43
44 potentiostat (PGSTAT10) controlled by Nova 1.5 software (Eco- 44
45 Chemie). The electrochemical cell, featuring a standard three- 45
46 electrode setup, was housed in an anaerobic glovebox ($\text{O}_2 < 2$ 46
47 ppm). The pyrolytic graphite edge (PGE) rotating disc working 47
48 electrode was used in conjunction with Pt wire as counter 48
49 electrode and a saturated calomel reference electrode (SCE) that 49
50 was housed in a Luggin sidearm. Potentials were converted to 50
51 the standard hydrogen electrode using the formula $E_{\text{SHE}} = E_{\text{SCE}}$ 51
52 $+ 0.241$ V at 25 °C.³⁰ All experiments were carried out under a 52
53 flow of high-purity gases (BOC) mixed using mass flow 53
54 controllers (Sierra instruments). The temperature (37 °C to 54
55

1 mimic, to the extent possible, the typical environment under 1
2 which the enzyme operates in its physiological host) was 2
3 controlled through a water jacket. All experiments were carried 3
4 out in mixed buffer³¹ adjusted to each pH value at 37 °C. The 4
5 working electrode was rotated at up to 2000 rpm to minimise 5
6 effects due to H_2 mass transport, although for scans at 1% H_2 it 6
7 proved impractical to overcome, completely, the diffusion 7
8 limitation for H_2 oxidation. 8

9 In a typical experiment, the PGE electrode was sanded with 9
10 P400 Tufbak sandpaper (Durite), rinsed and wiped with cotton 10
11 wool, then 5 μL enzyme solution (approximately 1 mg mL⁻¹) 11
12 was pipetted onto the surface of the graphite and left for 30 – 60 12
13 seconds to allow adsorption to occur. The working electrode 13
14 was then introduced to the cell containing the buffer and the 14
15 enzyme was activated by carrying out cyclic voltammetry scans 15
16 between -0.56 V and $+0.26$ V vs. SHE at 10 mV s⁻¹, under 100% 16
17 H_2 at pH 5, until the electrochemistry stabilised, before any 17
18 experiments were carried out. Cyclic voltammograms were 18
19 recorded and the forward and reverse scans were averaged to 19
20 help compensate for capacitive current. Where necessary, data 20
21 were smoothed using the Savitzky-Golay smoothing tool of 21
22 OriginPro 8.5.1 with a 25 mV window; in all cases, the smoothed 22
23 data were visually inspected to ensure they did not deviate from 23
24 the raw data. 24

25 We adopted the following procedure to distinguish trace 25
26 faradaic current due to low-level H^+ reduction activity above the 26
27 large capacitance current of the PGE electrode. A blank scan was 27
28 recorded with a bare PGE electrode under the same conditions 28
29 as the experimental scans. The average slope of two blank scans 29
30 (mean, $\pm (3\times \text{s.d.})$; $2.1 \times 10^7 \pm 6.85 \times 10^7$) served as a baseline 30
31 when analysing onset potentials for catalytic activity. We 31
32 reasoned that if reversible activity is occurring, the CV should 32
33 cut steeply across the zero-current (x -) axis at the equilibrium 33
34 potential E_{eq} ; hence the current-axis intercept marks the onset 34
35 of oxidation activity in this reversible case. For CVs in which 35
36 very little H^+ reduction activity is observed, the potential at 36
37 which the slope of the experimental scan exceeds the slope of a 37
38 blank scan is defined as the onset potential for oxidation 38
39 activity. 39

40 Results

41 Cyclic voltammograms recorded at pH 7.0, shown in Fig. 3A, 41
42 reveal that the onset of H_2 oxidation activity is unchanged as the 42
43 partial pressure of H_2 is varied over a 100 -fold range.²⁴ Conse- 43
44 quently, decreasing H_2 pressure has the effect of lowering the 44
45 overpotential requirement by raising the equilibrium potential 45
46 E_{eq} for the $2\text{H}^+/\text{H}_2$ couple (an increment of $+30$ mV per 10 -fold 46
47 decrease in $\rho(\text{H}_2)$). In contrast, the onset potential is clearly 47
48 affected by changes in pH (Fig. 3B). Under 100% H_2 , the onset 48
49 potential decreases by approximately 40 mV per pH unit in the 49
50 range pH 6 to 8, which is to be compared with the value of 61.5 50
51 mV per pH unit expected for the equilibrium potential E_{eq} . As a 51
52 result, the overpotential requirement decreases substantially as 52
53 the pH is lowered. 53

54 An ultimate result (Fig. 3C) is observed when cyclic voltam- 54
55 metry experiments are carried out at pH 3.0. Electrocatalysis at 55

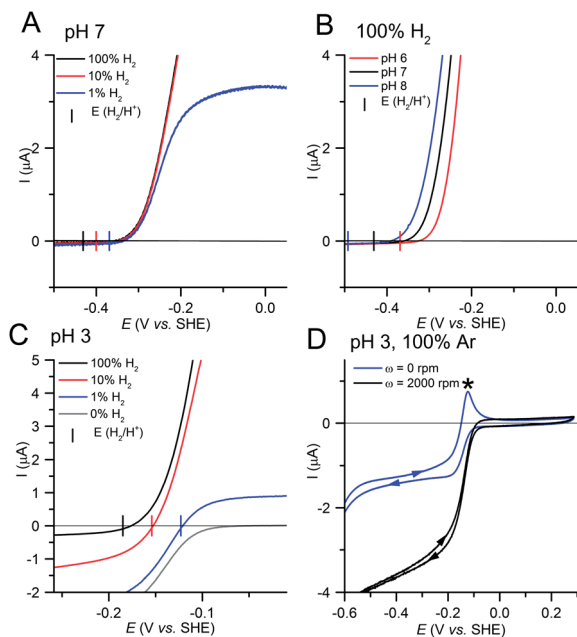


Fig. 3 Irreversible (A and B) and reversible (C and D) catalysis by *E. coli* Hyd-1. (A) At pH 7, changes in $\rho(\text{H}_2)$ have no effect on the onset potential. (B) Lowering the pH causes a 40 mV per unit shift in onset potential. (C) At low pH, the overpotential requirement for H_2 oxidation is minimised and current due to H^+ reduction becomes significant. (D) A comparison of voltammograms recorded at rotating and stationary electrodes at pH 3.0 confirm (prominent oxidation peak observed at stationary electrode) that the reductive current is due to H_2 production. All scans were recorded at 37 °C, scan rate 10 mV s^{-1} , electrode rotation rate (ω) 2000 rpm except in panel D. Scans in panels A–C have had background current subtracted.

low $\rho(\text{H}_2)$ now reveals a large current due to H^+ reduction and the voltammetry has become highly reversible; indeed, the current–potential trace intersects the potential axis sharply at values expected for E_{eq} at 1% H_2 or 10% H_2 , pH = 3.0, 37 °C. Under 100% H_2 the intersection potential is less well defined since the H^+ reduction current is much smaller, but the trend is still clearly marked, with E_{eq} becoming more positive by approximately 30 mV per decade increase in $\rho(\text{H}_2)$. A comparison of voltammograms obtained under stationary and rotating electrode conditions (Fig. 3D) confirms that the reduction current is due to H_2 production. For the stationary scan, H_2 production in the low-potential region leads to a build-up of H_2 at the electrode surface: the undisturbed H_2 is then re-oxidised as the potential crosses E_{eq} on the forward scan, giving rise to the sharp peak that is marked with an asterisk (*). This oxidation peak is not observed with rapid rotation of the electrode, which serves to disperse produced H_2 away from the electrode.

Fig. 4 gives a more complete demonstration of the changing properties of Hyd-1 as the pH is lowered. All voltammograms were recorded under 1% H_2 at a rotation rate of 2000 rpm and a scan rate of 10 mV s^{-1} . All experiments compared within a given figure were performed using the same enzyme film activated at pH 5.0 (see Methods) and then swapped between solutions of varying pH. The films were stable over time, allowing for direct comparison of the observed currents across conditions within an experiment (as

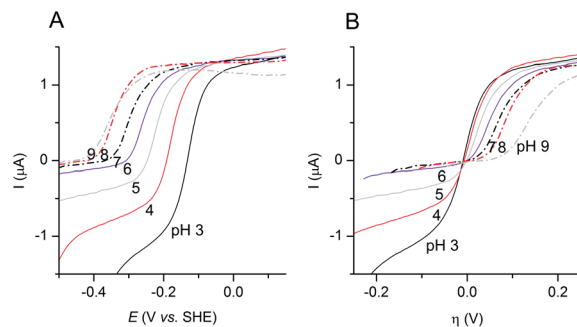


Fig. 4 Cyclic voltammograms of Hyd-1 at 1% H_2 , across a broad range of pH values. (A) Data are plotted as conventional current (I) vs. electrode potential (E) voltammograms. (B) Current traces are plotted as a function of overpotential. All scans were carried out at 37 °C, 1% H_2 , 10 mV s^{-1} , electrode rotation rate 2000 rpm.

mentioned later, Fig. S1† shows the enzyme is stable for at least two hours at pH 3, 37 °C). Panel A shows the standard current vs. potential traces, while panel B displays the same current traces as a function of the overpotential, $\eta = E - E_{\text{eq}}$ to allow for easy comparison of the overpotential requirement across different conditions. As the pH is lowered, the catalytic current for H_2 oxidation does not change significantly (it is diffusion-controlled under these conditions of low $\rho(\text{H}_2)$) whereas progressively more reduction current is obtained. Protein film electrochemistry rarely gives absolute activities because the minute amount of adsorbed electroactive enzyme is difficult to quantify; instead the technique records the relative activities in each direction. The sample of enzyme, being immobilised on the electrode surface, can easily be transferred between solutions of different pH. Under 100% H_2 (a condition under which H_2 oxidation is not diffusion-controlled) the H_2 oxidation current measured at +0.15 V for pH 3 was still approximately 50% of that measured at pH 6 for the same film (Fig. S2†). Panel B emphasises the link between overpotential requirement and catalytic bias: all scans exhibiting a significant overpotential requirement (*i.e.* those measured for pH \geq 6) also exhibit little to no H_2 production. Crucially, as the pH is lowered, the voltammetry increasingly resembles that of a standard [NiFe] hydrogenase or the classical reversible behavior of a Pt electrode. The tight correlation between the properties of overpotential requirement and lack of H_2 production in all scans further shows that the emergence of H^+ reduction activity is not due merely to increased H^+ availability at low pH but arises because Hyd-1 becomes a fundamentally more reversible catalyst under these conditions.

Establishing a quantitative definition for onset potential is difficult and various methods have been used:^{2,20,25} some papers do not describe the method by which onset potential is assessed,³² suggesting that it is assessed subjectively (by eye). The problem is that a PGE electrode has a high and complex resistance and capacitance, resulting in a charging current background that is very high compared to low-level Faradaic activity. We thus started from the simple observation that, in the potential region where catalytic turnover is very slow, the slope of the voltammogram is similar to the slope of a blank scan recorded under the same conditions, although the absolute value of the

current may differ slightly due to small variations from one experiment to another. The onset of rapid catalytic turnover is accompanied by a deviation of the voltammogram from the blank scan, *i.e.*, an increase in the slope of the experimental voltammogram relative to a blank voltammogram. We therefore defined the onset potential of activity as the potential at which the slope of an experimental voltammogram deviates from the slope of a blank scan (mean plus or minus $3 \times \text{s.d.}$). For scans in which reversible activity is observed, the CV passes steeply through the zero-current axis, and the intercept is therefore the point of 'onset'; the error due to a small current offset (*y*-axis) on the measured potential (*x*-axis) is minimised due to the steep slope of the voltammogram in this region.

Fig. 5 summarises the data collected over a range of pH values at both 1% and 100% H_2 (panels A and B). In panel C the onset potentials are portrayed as a function of pH, from which it is clear that for 1% H_2 and $\text{pH} < 5$ the onset potential values match the expected Nernstian equilibrium potentials, with a slope of $-61 \text{ mV per pH unit}$. For 100% H_2 the same is true except that the intersection potential is much less clearly defined and linearity is only just being approached at $\text{pH} 4$. As expected, the trendline at $\text{pH} < 4$ for 1% H_2 lies approximately 60 mV above that for 100% H_2 . As the pH is increased above $\text{pH} 5$, the onset potentials begin to deviate from the respective equilibrium potentials for the H^+/H_2 couple, the underlying trend being to become independent of H_2 concentration.

Comparative data were obtained for Hyd-2, the O_2 -sensitive 'standard' MBH produced by *E. coli* (Fig. S3†). For this enzyme, reversible electrocatalysis is observed at all pH values up to $\text{pH} 7$; scans at $\text{pH} 8$ show little to no H_2 production and the onset

potential does not move below -420 mV vs. SHE . Compared to Hyd-1, the stability of Hyd-2 to extremes of pH, both acidic and basic, is much decreased, as observed previously.³³ For Hyd-2, we see the same trend of increasing onset potential and loss of reversibility as E_{eq} becomes more negative – the difference between Hyd-1 and Hyd-2 being the pH (and thus the value of E_{eq}) at which this trend begins.

Assessment of the product inhibition constant during H^+ reduction, $K_{\text{I-app}}^{\text{H}_2/\text{H}^+}$ (Fig. S1†) for Hyd-1 shows that although product inhibition is significant ($K_{\text{I-app}}^{\text{H}_2/\text{H}^+} = 125 \mu\text{M}$ at $\text{pH} 3$, 37°C , -536 mV vs. SHE), it is of the same order as the previously published value for Hyd-2 ($K_{\text{I-app}}^{\text{H}_2/\text{H}^+} = 210 \mu\text{M}$ at $\text{pH} 6$, 30°C , -600 mV vs. SHE).²⁴ This experiment also serves as an excellent demonstration of the stability of Hyd-1 catalysis at low pH; the reductive current measured at the end of the two-hour experiment was more than 98% of the current recorded at the beginning of the experiment, under identical conditions.

One explanation that we must consider for the lack of H_2 production at high pH is that the enzyme undergoes an inactive–active transformation above a certain potential. At $\text{pH} 7$, this 'switch' potential would be well above E_{eq} , leading to the observation that only H_2 oxidation occurs, but at $\text{pH} 3$ the 'switch' potential could lie below E_{eq} allowing the enzyme to operate in reverse as long as the electrode potential does not become too negative. This behaviour is observed, for example, with succinate dehydrogenase, where the current due to fumarate reduction peaks within a narrow potential range then decreases.³⁴ A current peak is also observed for Hyd-1 and Hyd-2 as enzyme that has become oxidatively inactivated to form Ni-B (stable at high potential) undergoes reductive re-activation. Fig. S4† shows the waveshape expected were there to be a fast, potential-dependent active–inactive transformation that allowed H^+ reduction to occur within a narrow region of potential. If this transformation were slow, hysteresis would occur and voltammograms recorded over a range of scan rates would have different waveshapes. Fig. S5† shows a comparison of scans obtained for $\text{pH} 7$ and $\text{pH} 3$ (bidirectional), at 5 mV s^{-1} and 100 mV s^{-1} . There is clearly no evidence for an active–inactive transformation occurring in the potential range of interest.

Another possible source of overpotential would be a high reorganisation energy for the centre at which electrons enter or leave the enzyme, resulting in sluggish interfacial electron-transfer kinetics. In such a situation we expect to see an increased overpotential requirement for *both* directions of catalysis. Exploiting the ability of PFE to drive reactions at extremes of potential, it was established⁷ that no H^+ reduction current is evident at potentials as negative as -0.75 V (an overpotential of 0.35 V at $\text{pH} 7$). Therefore, a high reorganisation energy for interfacial electron transfer is not the cause of the high overpotential requirement observed for H_2 oxidation by Hyd-1.

Discussion

The results in this paper not only highlight the physical stability of an O_2 -tolerant [NiFe] hydrogenase under acidic conditions (significant because *E. coli* experiences a wide pH variation

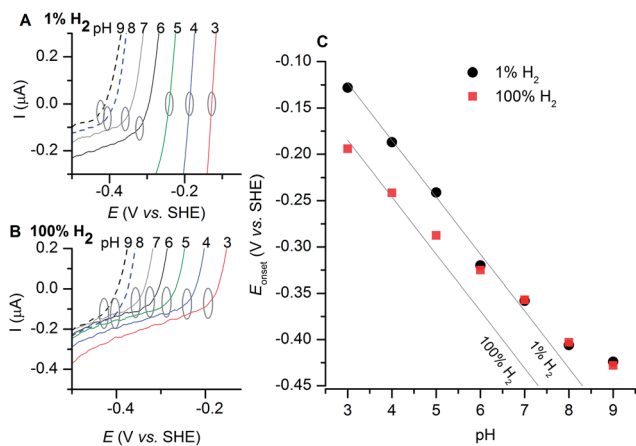


Fig. 5 Potential of H_2 oxidation onset as a function of pH and $\rho(\text{H}_2)$. All scans were carried out at 37°C , 10 mV s^{-1} , electrode rotation rate 2000 rpm . Panels A and B: close-up analysis of the electrocatalytic voltammograms for Hyd-1 as a function of pH at 1% H_2 (panel A) and 100% H_2 (panel B). The onset potential is defined as the zero-current intercept for scans in which significant reductive current is observable, and as the point at which the slope of the scan deviates from the average slope of a blank scan for CVs in which little to no reductive current is observed. Onset potentials are estimated to be accurate to within 0.01 V ; the ovals indicating onset potential are 0.02 V wide, indicating onset value \pm estimated error. Panel C shows the pH dependence of onset potentials, defined accordingly; grey diagonal lines indicate the value of E_{eq} .

during its passage through the gastrointestinal system) but also address the important question of what factors determine whether a hydrogenase is a good H₂ oxidiser or H₂ producer. In the specific case of Hyd-1, we have pursued the observation that when studied under neutral pH conditions, it acts *only* as an H₂ oxidiser and appears inactive at potentials below -0.3 V, even when no H₂ is present. Experiments undertaken over a wide range of pH values now show that *E. coli* Hyd-1 transforms into a fully reversible catalyst as the pH is lowered, with minimal overpotential requirement and high H⁺ reduction activity.

An analysis of how this shift in behaviour occurs helps us to understand why the electrocatalytic properties of O₂-tolerant MBHs seem to differ so substantially from standard hydrogenases. It is well known that [NiFe] hydrogenases are less proficient at H₂ evolution because of product inhibition. While this is particularly true for O₂-tolerant [NiFe] hydrogenases, the results (particularly the comparisons of $K_{1-app}^{H_2/H^+}$ values for Hyd-1 and Hyd-2 under relevant conditions) now reveal that product inhibition is *not* the reason for either the overpotential requirement for H₂ oxidation or the lack of reversibility at neutral pH.

The data presented in Fig. 3A and B show that at and above pH 6, the pH but *not* the partial pressure of H₂ shifts the onset potential of the oxidation wave. Since H₂ must bind and be transformed at the active site, the observation that the onset potential is unchanged over two orders of magnitude in H₂ partial pressure makes it highly unlikely that the overpotential requirement for H₂ oxidation (nearly 0.1 V at pH 7, 100% H₂) is due to a property of the [NiFe] catalytic site. In contrast to the lack of variation with $\rho(H_2)$, the onset potential shows a clear positive shift with decreasing pH but by a smaller degree than the corresponding shift in E_{eq} , hence the two values are converging. Indeed, as shown in Fig. 4B, there is a smooth transformation from irreversible to reversible electrocatalysis as the pH is lowered, which shows that the overpotential requirement for H₂ oxidation and the lack of H₂ production activity observed above pH 5 are closely related.

In a recent model for electrocatalysis,²⁸ Hexter *et al.* proposed that an important basis for the catalytic bias exhibited by an enzyme attached to an electrode surface is the difference between the reduction potential of the substrate redox couple (in this case H⁺/H₂) and the potential at which electrons enter or leave the catalytic cycle (the site at which this occurs is termed the electrochemical control centre³⁵). An analogous argument should hold for the enzyme's physiological activity where, for example, an electrode is replaced by the natural redox partner such as the quinone pool.³² The catalytic bias is minimised and reversibility maximised when the two potentials become close to one another, whereas the irreversible case is marked by a unidirectional current response with an onset defined by the reduction potential of the electrochemical control centre (ECC). The model allows us to explain the results of these experiments, because the substrate reduction potential E_{eq} shifts in a well-defined manner with pH (as required by thermodynamics) whereas the potential of the ECC is certain to have a milder pH dependence (as in this case) or no pH variation at all (as is typical for FeS clusters). The results highlight an interesting difference between enzymes and synthetic electrocatalysts:

redox enzymes usually possess relay centres that transport, trap and store charge – the ECC typically being one of these centres; in contrast, synthetic catalysts typically lack additional redox centres and the ECC must be the catalytic site itself. The *separation* of charge capture/transport and catalytic chemical conversions in enzymes suggests an important design principle for electrocatalysts in energy technologies.

Previous experiments carried out with proximal and medial cluster variants of Hyd-1 revealed that altering either cluster had a profound effect on the O₂ tolerance of the enzyme but no detectable effect on the onset potential for H₂ oxidation.^{6,7} Even in the case of a mutant in which residues at both the proximal and medial clusters were altered substantially, no change was seen in the bias or onset potential.⁷ We therefore consider it unlikely that the properties of either the proximal or medial clusters determine the bias and additional overpotential requirement. Having already argued that the [NiFe] site cannot be the source of the onset overpotential requirement, the simple process of elimination directs us to the distal cluster. The reduction potential of the distal [4Fe-4S] cluster should be insensitive to $\rho(H_2)$ because it does not interact with H₂, but it may be sensitive to pH depending on the extent to which acid-base equilibria involving nearby ionisable residues favour a particular oxidation level. Noting that histidine is one of the ligands to the distal [4Fe-4S] cluster it is possible that ionisation of the imidazole HN is influential, as with Rieske-type 2Fe-2S clusters.³⁶⁻³⁸ A dilemma here is that the distal [4Fe-4S] cluster in Hyd-1 appears silent to EPR spectroscopy, precluding direct determination of its reduction potential. The distal [4Fe-4S] cluster in the MBH of *R. eutropha* is similarly elusive: this problem is not restricted to hydrogenases, for example, complex I contains FeS clusters that are not detectable by EPR.³⁸⁻⁴¹

pH-dependent changes in the activity of various enzymes are commonly related to the pK_a value of amino acid residues directly involved in catalysis.⁷ However, in such a case, a departure from the pH close to the residue's pK_a should impair catalysis in both directions because (with the exception of residues positioned close to a redox centre) amino acid pK_a values are generally redox-insensitive. We thus exclude the possibility that the emergence of Hyd-1 H₂ production at low pH is due to a simple amino-acid ionisation effect.

The different catalytic bias for Hyd-1 and Hyd-2, as reflected in the sizeable onset overpotential requirement of Hyd-1 but not Hyd-2 under neutral pH conditions, is thus traced to an enzyme-based reduction potential. In general, notwithstanding the lack of information on the distal cluster of Hyd-1, the reduction potentials of FeS clusters in O₂-tolerant [NiFe] hydrogenases appear to be significantly more positive than for their O₂-sensitive counterparts. This feature results in more stable electron occupancy and greater ability to supply electrons back to the active site when O₂ attacks. A higher reduction potential for the distal cluster in O₂-tolerant MBHs would not only supplement this protection mechanism but also result in H₂ evolution being activated only at low pH.

Important remaining questions are whether the transformation in favour of H₂ production at low pH has any physiological or biotechnological significance. Both Hyd-1 (Fig. 5) and

Hyd-2 (Fig. S3†) show reversible catalysis at sufficiently low pH and irreversible catalysis at high pH; the difference is that Hyd-1 catalysis becomes irreversible above pH 5 whereas Hyd-2 catalysis only becomes irreversible above pH 8. As to a possible physiological link, several studies^{42,43} have shown that Hyd-2 is strongly expressed under mildly basic conditions (pH \approx 7.5) whereas Hyd-1 is more strongly expressed under acidic conditions (a pH value at least as low as 4.7). Both Hyd-1 and Hyd-2 project into the periplasm which, unlike the cytoplasm, is exposed to the external H⁺ environment. Thus if we compare these isoenzymes at their respective pH of maximal expression, they appear much more similar than they do at first glance, compared under identical conditions. The stability and H₂-evolution activity of Hyd-1 at pH 3, combined with the knowledge that Hyd-1 expression is up-regulated under acidic conditions, suggests that Hyd-1 is capable of environmental deacidification provided electrons are available from the quinol pool. Evidence suggests that Hyd-1 may act as a scalar proton pump during H₂ oxidation;^{29,32,44} consequently, H₂ production by Hyd-1 would require reverse electron transport and result in dissipation of the transmembrane proton gradient, an energetically costly process.

Several studies have provided compelling evidence that, in the absence of H₂ production by formate hydrogenlyase, both Hyd-1 and Hyd-2 can produce H₂ during an unusual type of anaerobic glycerol metabolism performed by *E. coli*, and H₂ production by Hyd-1 is maximised at low pH;^{45–47} importantly, *E. coli* fermentations commonly attain a pH well below 5.⁴⁸ The experiments we have now described, proving that Hyd-1 converts to an effective H₂ producer upon acidification and suggesting how this occurs, raise the possibility that H₂ production activity by Hyd-1 could serve as a physiological asset, particularly as *E. coli* transits through the gastrointestinal tract or is exposed to acid stress in the external environment. Finally, the demonstration that good rates of H₂ evolution are achievable with a highly O₂-tolerant [NiFe]-hydrogenase gives fresh impetus to the quest for practical and efficient biohydrogen production.

Acknowledgements

This research was supported by the Biological and Biotechnological Sciences Research Council (Grants BB/H003878-1 and BB/I022309-1). B.J.M. gratefully acknowledges the Oxford University Clarendon Fund and the Natural Sciences and Engineering Research Council of Canada for financial support. F.A.A. is a Royal Society-Wolfson Research Merit Award holder.

Notes and references

- 1 A. Volbeda, P. Amara, C. Darnault, J.-M. Mouesca, A. Parkin, M. M. Roessler, F. A. Armstrong and J. C. Fontecilla-Camps, *Proc. Natl. Acad. Sci. U. S. A.*, 2012, **109**, 5305–5310.
- 2 R. J. Maier, *Use of molecular hydrogen as an energy substrate by human pathogenic bacteria*, Portland Press, Colchester, UK, 2005.
- 3 J. W. Olson and R. J. Maier, *Science*, 2002, **298**, 1788–1790.

- 4 A. Parkin, C. Cavazza, J. C. Fontecilla-Camps and F. A. Armstrong, *J. Am. Chem. Soc.*, 2006, **128**, 16808–16815.
- 5 S. T. Stripp, G. Goldet, C. Brandmayr, O. Sanganas, K. A. Vincent, M. Haumann, F. A. Armstrong and T. Happe, *Proc. Natl. Acad. Sci. U. S. A.*, 2009, **106**, 17331–17336.
- 6 M. J. Lukey, M. M. Roessler, A. Parkin, R. M. Evans, R. A. Davies, O. Lenz, B. Friedrich, F. Sargent and F. A. Armstrong, *J. Am. Chem. Soc.*, 2011, **133**, 16881–16892.
- 7 R. M. Evans, A. Parkin, M. M. Roessler, B. J. Murphy, H. Adamson, M. J. Lukey, F. Sargent, A. Volbeda, J. C. Fontecilla-Camps and F. A. Armstrong, *J. Am. Chem. Soc.*, 2013, **135**, 2694–2707.
- 8 M. E. Pandelia, V. Fourmond, P. Tron-Infossi, E. Lojou, P. Bertrand, C. Léger, M. T. Giudici-Ortoni and W. Lubitz, *J. Am. Chem. Soc.*, 2010, **132**, 6991–7004.
- 9 M. E. Pandelia, P. Infossi, M. T. Giudici-Ortoni and W. Lubitz, *Biochemistry*, 2010, **49**, 8873–8881.
- 10 M. E. Pandelia, W. Nitschke, P. Infossi, M. T. Giudici-Ortoni, E. Bill and W. Lubitz, *Proc. Natl. Acad. Sci. U. S. A.*, 2011, **108**, 6097.
- 11 M.-E. Pandelia, P. Infossi, M. Stein, M.-T. Giudici-Ortoni and W. Lubitz, *Chem. Commun.*, 2012, **48**, 823–825.
- 12 M. M. Roessler, R. M. Evans, R. A. Davies, J. R. Harmer and F. A. Armstrong, *J. Am. Chem. Soc.*, 2012.
- 13 J. Fritsch, S. Loscher, O. Sanganas, E. Siebert, I. Zebger, M. Stein, M. Ludwig, A. L. De Lacey, H. Dau, B. Friedrich, O. Lenz and M. Haumann, *Biochemistry*, 2011, **50**, 5858–5869.
- 14 J. Fritsch, P. Scheerer, S. Frielingsdorf, S. Kroschinsky, B. Friedrich, O. Lenz and C. M. T. Spahn, *Nature*, 2011, **479**, 249–U134.
- 15 T. Goris, A. F. Wait, M. Saggu, J. Fritsch, N. Heidary, M. Stein, I. Zebger, F. Lenzian, F. A. Armstrong, B. Friedrich and O. Lenz, *Nat. Chem. Biol.*, 2011, **7**, 310–318.
- 16 J. Fritsch, O. Lenz and B. Friedrich, *Nat. Rev. Microbiol.*, 2013, **11**, 106–114.
- 17 K. A. Vincent, J. A. Cracknell, O. Lenz, I. Zebger, B. Friedrich and F. A. Armstrong, *Proc. Natl. Acad. Sci. U. S. A.*, 2005, **102**, 16951–16954.
- 18 A. F. Wait, A. Parkin, G. M. Morley, L. dos Santos and F. A. Armstrong, *J. Phys. Chem. C*, 2010, **114**, 12003–12009.
- 19 S. Krishnan and F. A. Armstrong, *Chem. Sci.*, 2012, **3**, 1015–1023.
- 20 L. Xu and F. A. Armstrong, *Energy Environ. Sci.*, 2013, **6**, 2166–2171.
- 21 B. Friedrich, J. Fritsch and O. Lenz, *Curr. Opin. Biotechnol.*, 2011, **22**, 358–364.
- 22 P. Chenevier, L. Mughlerli, S. Darbe, L. Darchy, S. DiManno, P. D. Tran, F. Valentino, M. Iannello, A. Volbeda, C. Cavazza and V. Artero, *C. R. Chim.*, 2013, **16**, 491–505.
- 23 J. A. Cracknell, K. A. Vincent, M. Ludwig, O. Lenz, B. Friedrich and F. A. Armstrong, *J. Am. Chem. Soc.*, 2008, **130**, 424–425.
- 24 M. J. Lukey, A. Parkin, M. M. Roessler, B. J. Murphy, J. Harmer, T. Palmer, F. Sargent and F. A. Armstrong, *J. Biol. Chem.*, 2010, **285**, 3928–3938.

- 1 25 G. Goldet, A. F. Wait, J. A. Cracknell, K. A. Vincent, M. Ludwig, O. Lenz, B. R. Friedrich and F. A. Armstrong, *J. Am. Chem. Soc.*, 2008, **130**, 11106–11113.
- 5 26 T. V. Laurinavichene, N. A. Zorin and A. A. Tsygankov, *Arch. Microbiol.*, 2002, **178**, 437–442.
- 27 R. M. Evans, A. Parkin, M. M. Roessler, B. J. Murphy, H. Adamson, M. J. Lukey, F. Sargent, A. Volbeda, J. C. Fontecilla-Camps and F. A. Armstrong, *J. Am. Chem. Soc.*, 2013.
- 10 28 S. V. Hexter, F. Grey, T. Happe, V. Climent and F. A. Armstrong, *Proc. Natl. Acad. Sci. U. S. A.*, 2012, **109**, 11516–11521.
- 29 A. Dubini, R. L. Pye, R. L. Jack, T. Palmer and F. Sargent, *Int. J. Hydrogen Energy*, 2002, **27**, 1413–1420.
- 15 30 A. J. Bard and L. R. Faulkner, *Electrochemical methods: fundamentals and applications*, Wiley, 2001.
- 31 A. K. Jones, S. E. Lamle, H. R. Pershad, K. A. Vincent, S. P. J. Albracht and F. A. Armstrong, *J. Am. Chem. Soc.*, 2003, **125**, 8505–8514.
- 20 32 R. W. Jones, *Biochem. J.*, 1980, **188**, 345–350.
- 33 R. G. Sawers and D. H. Boxer, *Eur. J. Biochem.*, 1986, **156**, 265–275.
- 34 J. Hirst, A. Sucheta, B. A. C. Ackrell and F. A. Armstrong, *J. Am. Chem. Soc.*, 1996, **118**, 5031–5038.
- 25 35 C. Leger, S. J. Elliott, K. R. Hoke, L. J. Jeuken, A. K. Jones and F. A. Armstrong, *Biochemistry*, 2003, **42**, 8653–8662.
- 36 I. J. Lin, Y. Chen, J. A. Fee, J. Song, W. M. Westler and J. L. Markley, *J. Am. Chem. Soc.*, 2006, **128**, 10672–10673.
- 37 A. R. Klungen and G. M. Ullmann, *Biochemistry*, 2004, **43**, 12383–12389.
- 38 Y. Zu, J. A. Fee and J. Hirst, *J. Am. Chem. Soc.*, 2001, **123**, 9906–9907.
- 39 K. Chen, C. A. Bonagura, G. J. Tilley, J. P. McEvoy, Y.-S. Jung, F. A. Armstrong, C. D. Stout and B. K. Burgess, *Nat. Struct. Mol. Biol.*, 2002, **9**, 188–192.
- 40 L. Forzi, J. Koch, A. M. Guss, C. G. Radosevich, W. W. Metcalf and R. Hedderich, *FEBS J.*, 2005, **272**, 4741–4753.
- 41 T. Leiding, K. Górecki, T. Kjellman, S. A. Vinogradov, C. Hägerhäll and S. P. Årsköld, *Anal. Biochem.*, 2009, **388**, 296–305.
- 42 P. W. King and A. E. Przybyla, *J. Bacteriol.*, 1999, **181**, 5250–5256.
- 43 K. Trchounian, C. Pinske, R. G. Sawers and A. Trchounian, *Cell Biochem. Biophys.*, 2011, 1–8.
- 44 J. Macy, H. Kulla and G. Gottschalk, *J. Bacteriol.*, 1976, **125**, 423–428.
- 45 K. Trchounian and A. Trchounian, *Int. J. Hydrogen Energy*, 2009, **34**, 8839–8845.
- 46 K. Trchounian, V. Sanchez-Torres, T. K. Wood and A. Trchounian, *Int. J. Hydrogen Energy*, 2011, **36**, 4323–4331.
- 47 K. Trchounian, B. Soboh, R. G. Sawers and A. Trchounian, *Cell Biochem. Biophys.*, 2012, 1–6.
- 48 A. Poladyan, A. Avagyan, A. Vassilian and A. Trchounian, *Curr. Microbiol.*, 2013, **66**, 49–55.